Quantum Electronics **41** (10) 886–894 (2011)

INTERACTION OF LASER RADIATION WITH MATTER. LASER PLASMA

PACS numbers: 52.50.Jm; 52.59.–f; 42.55.Lt
DOI: 10.1070/QE2011v041n10ABEH014688

Efficiency of generation of highly ionised atoms under resonance absorption of CO_2-laser radiation

S.Yu. Gus'kov, N.N. Demchenko, K.N. Makarov, V.B. Rozanov, Yu.A. Satov, B.Yu. Sharkov

Abstract. **We consider the generation of beams of highly ionised atoms in solid targets irradiated with CO_2-laser pulses. We present experimental results on generation of Mg and Pb ions from laser plasma at a radiation flux density $q \approx 10^{14}$ W cm^{-2}. We have developed a theoretical model describing the plasma heating by CO_2-laser radiation at a high pulse intensity on the target, taking into account the ponderomotive forces affecting the behaviour of the interaction of light with the plasma. It is shown that in the case of resonance absorption of laser radiation by the plasma, the efficiency of generation of highly ionised atoms of the target substance is higher than the efficiency of generation in the case of classical absorption. The results of the numerical calculation by the developed model are in good agreement with the experiment.**

Keywords: *CO_2 laser, highly ionised atoms, resonance absorption, fast electrons, fast ions.*

1. Introduction

Works, associated with generation of beams of highly charged ions, started in the 1960s within the framework of the fundamental research of plasma heated by intense laser pulses. In Russia, such studies were carried out at leading physics institutes [P.N. Lebedev Physics Institute (FIAN), A.M. Prokhorov General Physics Institute (IOFAN), Russian Federal Nuclear Center – The All-Russian Research Institute of Experimental Physics (RFNC – VNIIEF), National Research Centre 'Kurchatov Institute', Federal State Unitary Enterprise 'State Scientific Center of the Russian Federation – Institute for Theoretical and Experimental Physics' (ITEP), Federal State Unitary Enterprise 'State Research Center of the Russian Federation – Troitsk Institute for Innovation and Fusion Research' (TRINITI), National Research Nuclear University 'MEPhI' (MEPhI), etc.] using lasers of various types. In practical applications, the best justification was given to CO_2-based laser-plasma generators (LPGs) due to their relatively low cost, ecological compatibility of the technological scheme, and possible long-term operation in the frequency regime. The latter circumstance made it possible to successfully adapt the laser ion sources into injectors for charged-particle accelerators. Application of these injectors, for example, in the scheme of heavy ion synchrotrons, significantly simplifies the accelerator due to single (per pulse) filling of the ring by particles of the required mass and charge. Investigations of generation conditions of ions of different elements from the plasma heated by CO_2-laser pulses at flux densities up to $q \approx 3 \times 10^{13}$ W cm^{-2} and the development of LPGs of highly ionised atoms, intended for injection of charged particles in an accelerator, have been carried out at the ITEP and TRINITI within the framework of joint research programs [1–10]. In particular, it has been shown that for the efficient generation of many highly charged ions it is necessary, in addition to achieving a high density of the laser radiation flux, to match the laser pulse duration with the rate of plasma expansion – it must be less than the characteristic time of expansion. Thus, to maximise the number of particles with a higher degree of ionisation, shorter pulses are required. Based, in particular, on these physical studies, a high-current LPG of Pb^{25+} ions was designed and fabricated for the CERN accelerator [11]. The introduction of such a generator into the Large Hadron Collider (LHC) can significantly increase the energy of the accelerated particles used in the experiment.

Currently, further development of LPGs is carried out mainly within the framework of the ITEP scientific program on fundamental research of physics of high energy density in the matter, including joint projects with the FIAN. The problems formulated require the creation of LPGs of heavy ions with a significantly higher value of Z/A (Z is the degree of ionisation and A is the mass number of the element) and, accordingly, experiments at much higher laser power densities ($q \approx 10^{15} - 10^{16}$ W cm^{-2}). In these circumstances, the behaviour of interaction of radiation with plasma changes fundamentally. First of all, action of the ponderomotive force is accompanied by a change in the profiles of density and velocity of the plasma near the critical point. In addition, the size of the plasma inhomogeneity is greatly reduced, thereby leading to an increase in the range of angles of incidence of laser radiation at which resonant absorption takes place and fast electrons are generated. Indeed, the efficiency of resonance absorption is characterised by the function $\Phi(\tau)$, where $\tau = (k_0 L)^{1/3} \sin\theta_0$; k_0 is the wavenumber; L is the size of the plasma inhomogeneity; θ_0 is the angle of incidence. The range of τ values that are essential for resonance absorption, is $\Delta\tau \sim 1$, and the range of angles of incidence depends on the quantity

S.Yu. Gus'kov, N.N. Demchenko, V.B. Rozanov P.N. Lebedev Physics Institute, Russian Academy of Sciences, Leninsky prosp. 53, 119991 Moscow, Russia; e-mail: demch@sci.lebedev.ru;
Yu.A. Satov, B.Yu. Sharkov Federal State Unitary Enterprise 'State Scientific Center of the Russian Federation – Institute for Theoretical and Experimental Physics', ul. Bol'shaya Cheremushkinskaya 25, 117218 Moscow, Russia; e-mail: Yuri.Satov @ itep.ru;
K.N. Makarov Federal State Unitary Enterprise 'State Research Center of the Russian Federation – Troitsk Institute for Innovation and Fusion Research', ul. Pushkovykh 12, 142190 Troitsk, Moscow region, Russia

Received 5 July 2011; revision received 27 July 2011
Kvantovaya Elektronika **41** (10) 886–894 (2011)
Translated by I.A. Ulitkin

$(k_0L)^{1/3}$. The smaller the value of L, the larger the range of angles of incidence. A decrease in the size of the plasma inhomogeneity, on the one hand, increases the efficiency of resonance absorption and, on the other, suppresses the inverse bremsstrahlung absorption. In the vicinity of the critical point because of the dramatic changes in the plasma density at the transition from the supercritical to subcritical region there occurs a significant increase in the velocity of the ions due to the law of conservation of mass ρu = const. We will show below that the motion in the subcritical region is supersonic. Increasing the fraction of resonance absorption and, consequently, the fraction of energy carried by fast electrons, is accompanied by the emergence of the electric field at the plasma boundary, which accelerates the group of ions up to the velocities that are significantly higher than the characteristic hydrodynamic expansion velocity.

To date, interaction of high-power electromagnetic microwave and laser radiation with solid or gaseous targets have been studied in many experimental and theoretical works. Experiments associated with interaction of high-power microwave radiation with gas and plasma under resonance conditions were performed in 1970–1980s. These studies led to publication of monographs [12, 13].

2. Measurement technique and experimental results

Experiments on heating materials by CO_2-laser radiation and measurements of the characteristics of generated ions have been performed at the TRINITI using the setup described in [14]. The laser optical system made it possible to produce ~100-J pulses whose duration could be varied in the range from 15 to 30 ns. The laser beam with a diameter of 150 mm was directed into the vacuum chamber and focused onto the flat surface of a solid target with a spherical mirror lens $F/3$, in accordance with the scheme shown in Fig. 1. Time-of-flight measurements were performed in the direction of plasma expansion through a central opening in the objective of an axially symmetric optical axis and along the normal to the target. The power density, $q \approx 10^{14}$ W cm^{-2}, is estimated by measuring directly the size of the plasma glow in the X-ray spectral range and using diffraction calculations of the laser beam propagation, similar to those described in [11]. In analysing the charge composition, energy spectra, and partial ion currents, we used an electrostatic analyser of charged particles (spectral resolution $\delta E/E \approx 10^{-3}$) and a current collector, mounted at a distance of about 300 cm from the target. Raw data from the analyser were processed together with the signals of the total ion current, allowing the energy spectra of ion expansion to be reconstructed more accurately. Measurements of the individual signals of the spectrograph and the total current collector were fairly accurate, but the restoration of the entire spectrum required a series of measurements at different voltages of the analyser so that the error was determined by the data spread from shot to shot. The statistical spread of the data with the rms deviation of the mean was ±10% and ±25% for the current pulses and signals from the analyser, respectively. A detailed description of the instrumentation and data processing technique is given in [10, 15]. Figure 2 shows the averaged oscillograms of the ion current density for the Mg and Pb targets. This figure also presents the time dependence of the average degree of plasma ionisation, recovered from the data obtained in the measurements. Attention is drawn here to the fact that the value of the total ion current for a light element (compared to a heavy element) is much higher. Differences in the number of particles are even more significant (Fig. 3). Note also the large number of particles with a certain degree of ionisation generated in laser-produced plasmas. Thus, the percentage composition of He-like Mg^{10+} ions is 55%, and Pb^{25+} ions – 12% of the total number of particles. In addition to a highly charged group of ions generated at the stage of maximum heating of the plasma, a low charged group with significantly different characteristics of ions is subsequently produced [8]. This feature of ion generation in laser-produced plasma ensures the efficiency of the laser ion source in the injectors of charged particles. The energy spectra of

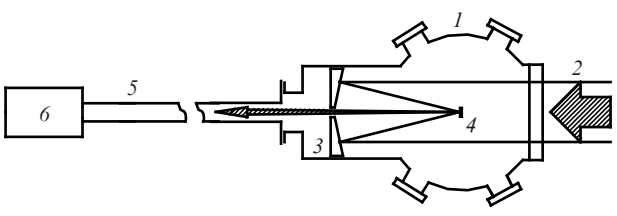

Figure 1. The scheme of irradiation of the target and time-of-flight measurements: (*1*) vacuum chamber; (*2*) laser beam; (*3*) mirror objective; (4) flat target; (*5*) drift tube; (*6*) current collector or energy analyser.

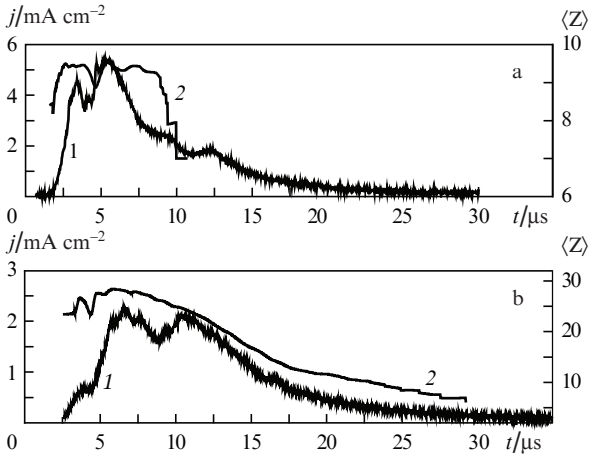

Figure 2. Oscillograms of signals of ion currents j (*1*) and the corresponding time dependences of the mean degrees of ionisation of plasma $\langle Z\rangle$ (*2*) for the elements of the targets made of Mg (a) and Pb (b).

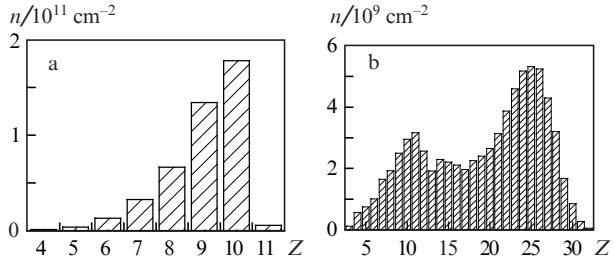

Figure 3. Dependence of the density of the number of particles normalised to the drift distance 1 m on the degree of ionisation of the targets made of Mg (a) and Pb (b).

expansion of magnesium and lead ions are shown in Figs 4 and 5. The spectrum of Mg^{8+} expansion (Fig. 4) is typical for the basic observed magnesium ions; it exhibits three groups of ions with a different slope of the distribution function: the first – in the range from 7 to 25 keV with a 'temperature' of ~3 keV, the second – in the range from 25 to 200 keV with a 'temperature' of ~30 keV, and the third – with energies above 200 keV and a 'temperature' of ~100 keV. The percentage content of the particles in these intervals is, respectively 59%, 39%, and 2% of their total number. The spectra of expansion of lead ions are more complex (Fig. 5): the 'cold' group of ions is observed only for ions with a relatively low charge multiplicity, such as Pb^{5+}; for ions with a higher charge multiplicity (Pb^{24+}) the spectrum exhibits only ions with a 'temperature' of several tens of keV and higher; and finally, the spectrum of maximally ionised ions (Pb^{30+}) is characterised by the 'temperature' above 100 keV.

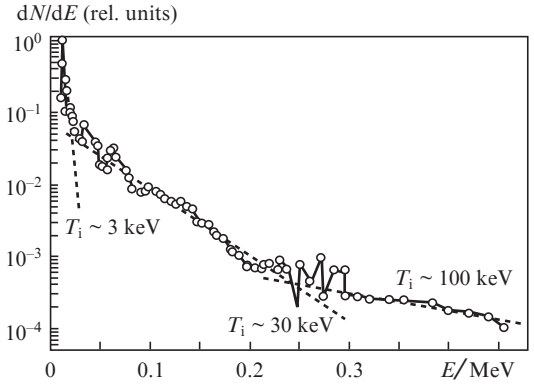

Figure 4. Energy spectrum of Mg^{8+} ions.

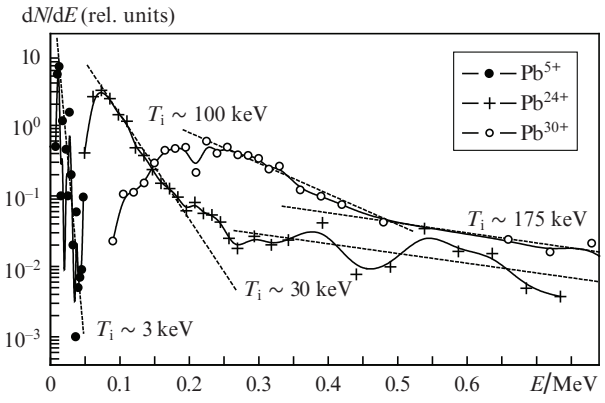

Figure 5. Energy spectra of Pb^{5+}, Pb^{24+}, Pb^{30+} ions.

3. Computational and theoretical model of interaction of laser radiation with plasma, taking into account the effect of ponderomotive force

Paper [16] deals with a theoretical model of interaction of the CO_2-laser pulse with plasma at flux densities no higher than 10^{12} W cm^{-2}, where the ponderomotive force can be neglected, and the relation between the mechanism of resonance absorption and acceleration of a small group of ions is considered. It was shown that fast electrons produced by resonance absorption, create an electric field that accelerates the group of ions to velocities significantly exceeding the velocity of hydrodynamic expansion. The efficiency of resonance absorption and energy of fast electrons depends on the size of the plasma inhomogeneity in the vicinity of the critical density $L = \rho_c(\partial\rho/\partial z)_c^{-1}$, where ρ is the plasma density, ρ_c is the critical density, and the z axis is directed along the density gradient. The amplitude of the longitudinal electric field at the critical point is found from the expression [17]:

$$|E_{zc}| = \frac{|H_0|\,\Phi(\tau)}{(2\pi k_0 L)^{1/2}\varepsilon_2}, \tag{1}$$

where $|H_0|$ is the field amplitude of the incident wave (in the incident wave the amplitudes of the electric and magnetic fields are equal); $\Phi(\tau) = 4\tau V(\tau^2)[V(\tau^2)/(-V'(\tau^2))]$ (see, e.g., [17]); V and V' are the Airy function and its derivative; $\tau = (k_0L)^{1/3}\sin\theta_0$; θ_0 is the angle of incidence; ε_2 is the imaginary part of the plasma permettivity at the critical point. The function $\Phi(\tau)$ with good accuracy (the maximum error does not exceed 10%) can be written in the form

$$\Phi(\tau) \approx \frac{2\tau}{\sqrt{\tau^2 + 0.46}}\exp\left(-\frac{2}{3}\tau^2\right). \tag{2}$$

The contribution of electron–ion collisions into ε_2 in formula (1) in our case is negligible due to the low critical plasma density. The longitudinal field under the resonance absorption is limited either due to the energy ejection by the plasma waves if the amplitude of the electron oscillations $a_{os} = e|E_{zc}| \times (m_e\omega^2)^{-1}$ in this field is smaller than the resonance width $\varepsilon_2 L$, or due to the energy ejection by fast electrons if a_{os} exceeds the width of the resonance. In the case of limitation by the plasma waves [17]

$$\varepsilon_2 = \varepsilon_{2p} = \left(\frac{\beta_T}{k_0 L}\right)^{2/3}, \tag{3}$$

where $\beta_T = [T_e/(m_e c^2)]^{1/2}$, T_e is the electron temperature. In the case of limitation by the current of fast electrons [16]

$$\varepsilon_2 = \varepsilon_{2h} = \left(\frac{e\alpha_0\,|H_{yc}|}{\pi m_e\omega^2 L}\right)^{1/2}, \tag{4}$$

where $\alpha_0|H_{yc}| = |H_0|\Phi(\tau)/(2\pi k_0 L)^{1/2}$, $|H_{yc}|$ is the magnetic field amplitude at the critical point.

The energy of fast electrons can be estimated as the energy of the electron oscillations in a resonant field $\mathcal{E}_h = e^2|E_{zc}|^2 \times (m_e\omega^2)^{-1}$. As will be shown below, this energy for the considered conditions far exceeds T_e. In this case, the electron distribution function describes the electron beam in plasma, which relaxes in a collisionless manner due to generation of plasma waves. In the opposite case, when the oscillation energy is less than T_e, we deal with the diffusion of the electron distribution function to higher energies due to collisionless damping of plasma waves by the electrons. In this case, the energy of fast electrons can considerably exceed the energy of oscillations.

The efficiency of resonance absorption is $\delta_a^r \sim \Phi^2(\tau)$. The maximum value is $\delta_a^r \approx 0.5$ at $\tau \approx 0.7$ [18]. With increasing the laser radiation flux density, the density gradient at the critical point will be determined by the ponderomotive force (ε_1 –

$1)\nabla|E|^2/(16\pi)$, where $\varepsilon_1 = 1 - \rho/\rho_c$ is the real part of the permettivity of plasma. The ponderomotive force can be expressed as the gradient of the ponderomotive potential p_r, which in the hydrodynamic equation of motion is added to the thermal plasma pressure. To this end, we consider Maxwell's equations in the case of a p-polarised wave having a frequency ω [time dependence $\sim\exp(-i\omega t)$]. Let the z axis be directed along the density gradient, and the (y, z) plane be the plane of incidence. Then the field components E_y, E_z and H_x are nonzero. Maxwell's equations can be written in the form

$$\frac{dE_y}{dz} = -ik_0\frac{\varepsilon - \alpha_0^2}{\varepsilon}H_x, \tag{5}$$

$$\frac{dH_x}{dz} = -ik_0\varepsilon E_y, \tag{6}$$

$$E_z = \frac{\alpha_0}{\varepsilon}H_x. \tag{7}$$

Here $\alpha_0 = \sin\theta_0$, $\varepsilon = \varepsilon_1 + i\varepsilon_2$ is the complex permettivity. The field structure is determined mainly by the real part ε_1. The imaginary part describes the weak (within one wavelength) amplitude damping due to absorption of radiation, and also eliminates the singularity at the critical point in (7) for the longitudinal field. In the case of weak absorption (within one wavelength), the imaginary part ε can be neglected and expressions (5) – (6) yield the relation

$$\varepsilon\frac{d|E_y|^2}{dz} = -\frac{\varepsilon - \alpha_0^2}{\varepsilon}\frac{d|H_x|^2}{dz}. \tag{8}$$

To do this, we multiply (5) by E_y^*, and the equation, that is complex conjugate of (5), by E_y, and then add up the obtained equations. Proceeding in a similar manner with equation (6), which we first multiply by H_x^* and H_x and then add up the obtained results, we obtain expression (8). Using (8) we can derive

$$(\varepsilon - 1)\frac{d}{dz}(|E_y|^2 + |E_z|^2) = -\frac{d}{dz}[|E_y|^2 + |H_x|^2 + (1 - 2\varepsilon)|E_z|^2]. \tag{9}$$

Consequently, in the case of p-polarisation, the ponderomotive pressure is written as

$$p_r = \frac{1}{16\pi}[|E_y|^2 + |H_x|^2 + (1 - 2\varepsilon)|E_z|^2]. \tag{10}$$

At angles of incidence that are not close to zero, the longitudinal field $|E_z|$ near the critical point according to (7) is significantly higher than the other terms in (10):

$$|E_z|^2 = \frac{\alpha_0^2|H_x|^2}{(1 - \rho/\rho_c)^2 + \varepsilon_2^2}, \tag{11}$$

where $\varepsilon_2 = \nu/\omega$ (in the expression for ε_2 we assume that ω is equal to the plasma frequency ω_p); ν is the effective frequency of the field energy dissipation in the resonance region related either to generation of plasma wave (3), or to generation of fast electrons (4). The maximal $|E_z|^2$ is achieved at the critical point. According to (10), if we take into account only the term with $|E_z|^2$, the maximum p_r occurs at a density that is slightly different from the critical point. This difference is insignificant ($\Delta\rho/\rho_c \approx \nu/\omega$) and due to the fact that in deriving (10), we considered a real ε. However, the singularity in (7) is eliminated by the imaginary part. Because of the small differences between the densities at which the maximal $E_z|^2$ and p_r are achieved, this issue is not important for further conclusions.

Because the spatial scale of variation in the density profile, caused by the ponderomotive force in the field of the critical density, is very small (of the order of the laser radiation wavelength), the motion of the plasma in this narrow region can be described using the stationary equations of continuity and motion under the assumption of constant electron and ion temperatures:

$$\rho u = \rho_c u_c, \tag{12}$$

$$\rho u\frac{du}{dz} = -\frac{dp_T}{dz} - \frac{\rho}{16\pi\rho_c}\frac{d|E|^2}{dz}, \tag{13}$$

where u is the velocity of plasma with respect to the critical surface; $p_T = \rho c_s^2$ is the thermal pressure; $c_s = [(ZT_e + T_i)\times m_i^{-1}]^{1/2}$ is the isothermal velocity of ion sound (m_i is the ion mass); the right-hand side of (12) contains the quantities taken at the critical point. By using (12), equation (13) transforms as

$$(c_s^2 - u^2)\frac{d\rho}{dz} = -\frac{\rho}{16\pi\rho_c}\frac{d|E|^2}{dz}. \tag{14}$$

This equation implies that the critical point is sonic ($u_c = c_s$), because $|E|^2$ has a maximum at the critical point, and $(d\rho/dz)_c$ is nonzero. According to (14) the subcritical plasma is supersonic, and the motion at $\rho > \rho_c$is subsonic. Using expression (10) for the ponderomotive pressure, instead of equation (13) we can write the law of conservation of momentum:

$$p_T + p_r + \rho u^2 = 2\rho_c c_s^2 + p_{rc}. \tag{15}$$

Let ρ_1 be the density of the supercritical plasma, where $p_r \to 0$. For the ratio ρ_1/ρ_c we can obtain from (12) and (15)

$$\frac{\rho_1}{\rho_c} = \left(1 + \frac{\delta}{2}\right) + \sqrt{\delta + \frac{\delta^2}{4}}, \tag{16}$$

where $\delta = p_{rc}/(\rho_c c_s^2)$ is the ratio of the ponderomotive pressure at the critical point to the heat pressure. If in the critical point $|E_z|^2$ is considerably higher than other terms in (10) (in this case, the angle of incidence should not be very close to zero), then in the subcritical region we can also set $p_r = 0$. Then, similarly to expression (16), for the subcritical density ρ_0 we have

$$\frac{\rho_0}{\rho_c} = \left(1 + \frac{\delta}{2}\right) - \sqrt{\delta + \frac{\delta^2}{4}}. \tag{17}$$

If $\delta \gg 1$, then $\rho_1/\rho_c \approx \delta$ and $\rho_0/\rho_c \approx 1/\delta$. Accordingly, the supercritical plasma velocity is $|u_1| \approx c_s/\delta$, and the velocity in the subcritical region is $|u_0| \approx \delta c_s$ (the sign of the velocity is negative because the motion occurs in the opposite direction to the z axis).

Expressions (16), (17) determine the magnitude of the density jump in the critical region in the absence of viscous pressure of the ions. To determine the scales of the plasma inhomogeneity at the critical point, it is necessary to consider the equation that defines the structure of the jump. To do this, the equation of motion should take into account the ion viscosity $p_v = -\mu\partial u/\partial z$. Then, instead of (15) we have

$$p_T + p_r + \rho u^2 - \mu\frac{du}{dz} = 2\rho_c c_s^2 + p_{rc} + p_{vc}. \quad (18)$$

The critical point is sonic in this case, because the derivative du/dz has a maximum at the critical point, and, therefore, $(d^2u/dz^2)_c = 0$. As a result, we arrive at (14). With the help of (12), equation (18) can be written in the form

$$\frac{a}{x^2}\frac{dx}{dz} = \left(\frac{1}{x} + x - 2\right) + \beta(x), \quad (19)$$

where $a = \mu/(\rho_c c_s)$, $x = \rho/\rho_c$, $\beta(x) = [p_r(x) - p_{rc} - p_{vc}]/(\rho_c c_s^2)$. The right-hand side of (19) determines the sign of the derivative of the density x, which should not be negative. The function $F(x) = 1/x + x - 2$ has a minimum, equal to zero, at $x = 1$. The function $\beta(x)$ at the critical point is positive and determined by the constant $(-p_{vc})$ (p_{vc} is negative because $u < 0$ and $du/dz > 0$). The sum $F(x) + \beta(x)$ has a minimum at $x > 1$. It is essential that in the minimum this sum vanishes, which yields the asymptote for the solution $x(z)$. If the sum $F(x) + \beta(x)$ in the minimum is negative, then we obtain two values x_1 and x_2, for which this sum is zero. Let $x_2 > x_1$, then the transition from the density x_1 to x_2 should occur abruptly, which is unacceptable in the presence of viscosity (viscous pressure tends to infinity). Since the function $\beta(x)$ is narrow compared to $F(x)$ (changes more rapidly along the x axis), the condition for the nonnegativity of the right-hand side of (19) can be approximately written as $-p_{vc} \approx p_{rc}$, or

$$|p_{vc}| \approx \frac{|E_{zc}|^2}{16\pi}. \quad (20)$$

Consider the possible mechanisms of dissipation of ion perturbations that determine the viscosity coefficient μ. There is an expression for the coefficient of the ion viscosity due to ion–ion collisions [19]: $\mu = 0.48\rho v_{Ti}/\nu_{ii}$, where v_{Ti} is the thermal velocity of ions, and ν_{ii} is the Coulomb frequency of ion–ion collisions. The expression for the collisionless damping decrement of ion perturbation on the electrons in a nonisothermal plasma is also known at $T_e \gg T_i$ [20]. As will be shown below, in a plasma moving under a significant ponderomotive force there arises another case of nonisothermalily, where $T_i \gg T_e$ [21]. Such a state is perhaps due to the fact that the coefficients of the ion and electron thermal conductivities differ significantly (the coefficient of the ion thermal conductivity is smaller), and a higher ion temperature is required to transfer the energy by the ions into a dense part of the target. In this case, the ion heating is due to the dissipation of ion perturbances caused by the ponderomotive force. Therefore, the expression for the collisional viscosity is usually not applicable due to the fact that the mean free path of an ion becomes larger than the ion plasma inhomogeneity. However, when $T_i \gg T_e$, there appears an effective mechanism of collisionless damping on the ions. When $T_e \gg T_i$, damping on the ions can be neglected, because the number of ions involved in damping is exponentially small (these ions are located in the tail of the Maxwellian distribution function); ion perturbations damp on the electrons, despite the fact that the ion pre-exponential factor of the imaginary part of the permettivity is $(m_i/m_e)^{1/2}$ times greater than the electron factor. A different situation arises when $T_i \gg T_e$. In this case, the ion exponential factor in the imaginary part of the permettivity is not small, and there arises strong damping of perturbations on the ions. Note that in the case of weak damping of perturbations (when $T_e \gg T_i$) the scales of the plasma inhomogeneity can be determined by taking into account the dispersion, described by the Korteweg–de Vries equation. In this case, equation (18) should contain the term with the second derivative of the velocity in z, and the left-hand side of equation (19) – the term $(r_D^2/2)d^2(1/x)/dz^2$ [20] (r_D is the Debye radius), because according to (12), the velocity is proportional to $1/x$. As will shown below, when $T_i \gg T_e$, dissipation leads to the inhomogeneity size L, which is significantly greater than the Debye radius; therefore, the dispersion term is only a small addition of the order $(r_D/L)^2$ to the dissipative one. Unlike the dispersion structure of the plasma motion described by the Korteweg–de Vries equation, the case considered here is naturally called the dissipative structure of the plasma motion.

Collisionless dissipation on the ions occurs in a slow (longitudinal) field E_s, which is produced by the ponderomotive force in the plasma. In the more general case, the slow field is also determined by the thermal pressure of electrons according to the equation

$$en_eE_s = -\frac{dp_{Te}}{dz} - \frac{\rho}{16\pi\rho_c}\frac{d|E_z|^2}{dz}. \quad (21)$$

However, we assume here that the energy of electron oscillations in the high-frequency resonance field is greater than the thermal energy T_e, and in (21) we omit the term with the thermal pressure. Using expression (11) for $|E_z|^2$, we can find the maximum value of the derivative $d|E_z|^2/dz$ and express it through the value of the field $|E_z|_c$ at the critical point:

$$\left(\frac{d|E_z|^2}{dz}\right)_m = |E_z|_c^2\frac{3\sqrt{3}}{8}\frac{1}{\varepsilon_2\rho_c}\frac{d\rho}{dz}.$$

Then, for the slow field maximum, we obtain from (21)

$$E_{sm} = \frac{3\sqrt{3}\,m_i|E_z|_c^2}{128\pi eZ\rho_c^2\varepsilon_2}\frac{d\rho}{dz}. \quad (22)$$

To determine the effective viscosity μ, we will equate two expressions for the rate of dissipation of kinetic energies of the ions:

$$\frac{\sigma_s|E_{sm}|^2}{2} = \mu\left(\frac{du}{dz}\right)^2. \quad (23)$$

Here $\sigma_s = \omega_s\varepsilon_{s2}/(4\pi)$ is the ion conductivity in a slow field; $\omega_s = k_s c_s$, ε_{s2} is the imaginary part of the permettivity caused by the ions. Strictly speaking, the transition layer is a wave packet with different ω_s and k_s. At this stage, we will restrict or consideration to the assessment that takes into account only one characteristic harmonic with $k_s \approx 1/\Delta_r$, where $\Delta_r = L\varepsilon_2$ is the width of the resonance. From (23) we obtain

$$\mu = \frac{27\omega_s\varepsilon_{s2}m_i^2p_{rc}^2}{512\pi e^2Z^2\rho_c^2c_s^2\varepsilon_2^2}, \quad (24)$$

where $p_{rc} = |E_z|_c^2/(16\pi)$. The expression for $\omega_s\varepsilon_{s2}$ has the form [20]

$$\omega_s\varepsilon_{s2} = \sqrt{\frac{\pi}{2}}\frac{\omega_s^2\omega_i^2}{(k_sv_{Ti})^3}\exp\left(-\frac{\omega_s^2}{2k_s^2v_{Ti}^2}\right). \quad (25)$$

Here, $\omega_i = (4\pi Z^2 e^2 n_i/m_i)^{1/2}$ is the ion plasma frequency. Given the condition (20), i.e., the equality $|p_{vc}| = p_{rc}$, as well as writing the viscous pressure in the form $p_{vc} = -\mu c_s/L$, we can obtain from (24) another expression for the viscosity coefficient:

$$\mu = \frac{128\rho_c\omega_i^2\varepsilon_2^2 L^2}{27\omega_s\varepsilon_{s2}}. \quad (26)$$

Comparing this expression with the expression for the collisional viscosity, we may note that in the collisionless case quantities $\omega_i\Delta_r$ and $\omega_s\varepsilon_{s2}$ play the roles of the thermal velocity of ions and the frequency of collisions, respectively.

The equation for determining the inhomogeneity size L is derived from equation (20), when writing the viscous pressure in the form $\mu c_s/L$. Next, we consider the case when the field in the resonance is limited by plasma waves, i.e., $\varepsilon_2 = \varepsilon_{2p}$ according to (3). Then, to determine the k_0L, we have the equation

$$(k_0L)^{4/3} = \frac{32\pi^2\beta_T^{4/3}k_0c_s\mu}{\Phi^2|H_0|^2}. \quad (27)$$

In (27), the functions μ and Φ also depend on k_0L. The function $\Phi(\tau)$ for $\tau < 0.7$ can be approximately written as $\Phi \approx 2.95\tau = 2.95\alpha_0(k_0L)^{1/3}$. Using also expression (26) for μ, we can derive a formula for calculating k_0L:

$$(k_0L)^{5/3} = \frac{4096\sqrt{2}\pi^{3/2}\rho_c\beta_T^{2/3}v_{Ti}^3}{27\times 2.95^2\alpha_0^2|H_0|^2c_s}\exp\left(\frac{c_s^2}{2v_{Ti}^2}\right). \quad (28)$$

In addition to the inhomogeneity size at the critical point, it is important to know the values of the plasma density at the boundaries of the transition layer: $x_0 = \rho_0/\rho_c$ is the dimensionless density in the subcritical region, and $x_1 = \rho_1/\rho_c$ – in the supercritical region. The densities x_0 and x_1 can be found from the condition of minimum of the right-hand side of (19), i.e., the minimum of the sum $F(x) + \beta(x)$. Equating the derivative $F'(x) + \beta'(x)$ to zero and neglecting the quantity ε_2^2 in comparison with $(1 - x)^2$, we obtain the equation

$$(x + 1)(x - 1)^4 = 2bx^2, \quad (29)$$

where $b = p_{r0}\Phi^2/(4\pi\rho_c c_s^2 k_0 L)$, $p_{r0} = |H_0|^2/(8\pi)$ is the light pressure in the incident wave. An approximate solution of equation (29) for $x \gg 1$ is found by writing it in the form $(x - 1)^3 = 2bx^2/(x^2 - 1)$ and setting $x^2/(x^2 - 1) \approx 1$. Then, in the supercritical region we have the solution $x_1 \approx 1 + (2b)^{1/3}$. If x is small, we can use the method of successive approximations, calculating new values of $x^2/(x^2 - 1)$. When $x \ll 1$, the solution is obtained by setting $(x + 1) \approx 1$ in (29). The solution has the form $x_0 = (1 + c/2) - [(1 + c/2)^2 - 1]^{1/2}$, where $c = (2b)^{1/2}$. In this case, we can also use the method of successive approximations, calculating new values of $(x + 1)$. The values of x_0 and x_1 depend on the parameter b, which is proportional to the ratio of light pressure in the incident wave to the thermal pressure of plasma at the critical point. The above approximate solutions for x_0 and x_1 are valid for large b. At small light pressures ($b \ll 1$), when $x \approx 1$, but nevertheless $(x - 1)^2 > \varepsilon_2^2$, we can set $(x + 1) \approx 2$ in (29). Then, for x_0 and x_1 we obtain

$$x_{1,0} = \left(1 + \frac{c_1}{2}\right) \pm \sqrt{\left(1 + \frac{c_1}{2}\right)^2 - 1}, \quad (30)$$

where $c_1 = b^{1/2}$.

Consider the problem of interaction of the CO_2-laser pulse with a titanium target at a laser radiation flux density of 10^{14} W cm^{-2} and a FWHM pulse duration of 20 ns (the diameter of the focal spot is 65 μm). The focusing system ensures the maximum angle of incidence, 9°. In general, even in the case of an axially symmetric laser beam, the problem on its interaction with the target is three dimensional, because the polarisation in the beam is linear, and the component of the electric field along the density gradient depends on the azimuthal angle φ as $\cos\varphi$. Because the square of the field depends on the angle φ as $\cos^2\varphi$, in calculating the fraction of resonance absorption we should take into account the fact that only half of the incident flux is p-polarised (the average value of $\cos^2\varphi$). As was already mentioned above, the region of a sharp change in the density profile in the vicinity of the critical density is narrow, and we can reduce the general problem to a simpler problem of plane motion of the plasma under oblique incidence of p-polarised radiation. For this purpose, we performed numerical calculations using a one-dimensional hydrodynamic RAPID-SP code [21], in which laser radiation is considered in the framework of Maxwell's equations. This code takes into account the ponderomotive force and oblique incidence of electromagnetic waves of any polarisation on the plane-layered plasma, uses an analytical model for generation of fast electrons under resonance absorption, and considers the energy transfer by fast electrons, while the equation of state takes into account the energy loss due to plasma ionisation. Because we studied the small-scale motion of the plasma, the laser flux density of 10^{14} W cm^{-2} can be assumed constant in time. Radiation was p-polarised, and the angle of incidence was varied. Figure 6 presents the calculated profiles of density, temperature and plasma velocity, as well as the square of the electric field amplitude at the instant 0.2 ns after the pulse onset. The angle of incidence was 30°. The figure also shows a sharp transition from the supercritical density region to the

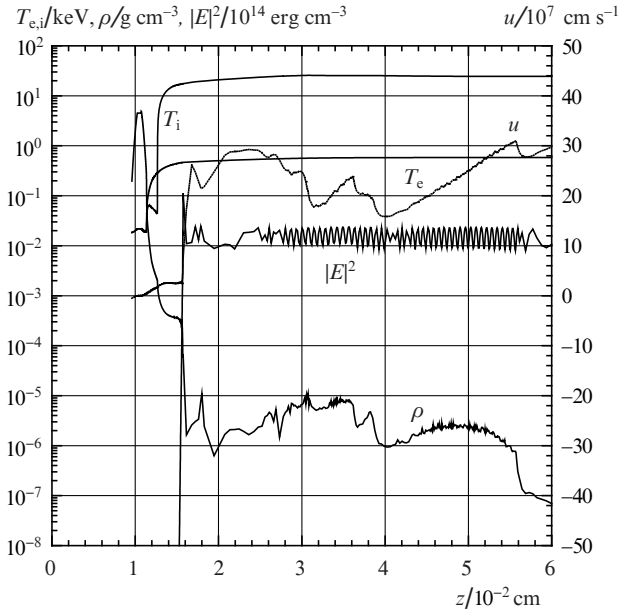

Figure 6. Profiles of density ρ, velocity u, electron and ion temperatures T_e and T_i, and the square of the electric field amplitude $|E|^2$ at an instant 0.2 ns after the pulse onset. Laser radiation at a wavelength of 10.6 μm is incident from the right (the flux density, 10^{14} W cm^{-2}; angle of incidence, 30°; p-polarisation).

subcritical one (for titanium $\rho_c = 4.09 \times 10^{-5}$ g cm^{-3}). Accordingly, the plasma velocity increases in the subcritical region. The ion temperature is much higher than the electron temperature due to the viscous heating of ions and the large difference in coefficients of thermal conductivity of electrons and ions (the electron coefficient is higher). Table 1 shows the values of the fraction of total absorption δ_a (inverse bremsstrahlung and resonance mechanisms) and the fraction of resonance absorption δ_a^r as a function of the angle of incidence. The values of $\delta_a$and δ_a^r are given for a 0.5-ns pulse. It follows from Table 1 that absorption mainly arises due to the resonance mechanism. The ponderomotive force leads to a decrease in the efficiency of inverse bremsstrahlung absorption and to an increase in the fraction of resonance absorption. Using the hydrodynamic ATLANT-HE code [22] we also carried out a two-dimensional calculation of interaction of a 20-ns pulse with a titanium target at the flux density of 10^{14} W cm^{-2}. This calculation allowed us to determine the fraction of resonance absorption for a real focusing system after the laser pulse terminates.

Table 1.

θ_0/deg	δ_a	δ_a^r
15	0.268	0.254
30	0.508	0.491
45	0.502	0.482

To estimate the field in the resonant absorption region and the energy of fast electrons, we set $T_e = 0.55$ keV and $T_i = 20$ keV (these values were obtained in a one-dimensional calculation at an angle of incidence $\theta_0 = 9°$). With the help of (28), we have $k_0L = 5.95$, $L = 9.92$ μm, $\alpha_0|H_c| = \Phi|H_0|/\sqrt{2\pi k_0 L} = 1.25 \times 10^5$ CGS units, $|H_0| = 9.15 \times 10^5$ CGS units. The imaginary part of the permettivity $\varepsilon_{2p} = 0.0312$, the square of the field amplitude $|E_{zc}|^2 = 1.61 \times 10^{13}$ CGS units, the energy of fast electrons $\mathcal{E}_h = 78.5$ keV. The solution of equation (29) by the method of successive approximations yields $x_0 = 0.72$, $x_1 = 1.36$. Hence, due to ponderomotive acceleration, ions acquire a velocity relative to the critical surface, $c_s/x_0 = 3.45 \times 10^7$ cm s^{-1}.The numerical calculation also allowed us to determine the velocity of the critical surface motion towards the incident laser pulse, which during the time 0.4–1.0 ns increases from 3.11×10^7 to 4.82×10^7 cm s^{-1}. Consequently, in the laboratory coordinates the ion velocity reaches 8.27×10^7 cm s^{-1} ($\mathcal{E}_i = 170$ keV).

Consider the conditions for emergence of the isothermal plasma with $T_i \gg T_e$. To this end, we use the energy equation of electrons and ions in the Lagrangian variables (m, t):

$$\frac{\partial \mathcal{E}_e}{\partial t} = -p_{Te}\frac{\partial u}{\partial m} - \frac{\partial q_{Te}}{\partial m} - Q_{ei}(T_e - T_i), \tag{31}$$

$$\frac{\partial \mathcal{E}_i}{\partial t} = -\pi_i\frac{\partial u}{\partial m} - \frac{\partial q_{Ti}}{\partial m} + Q_{ei}(T_e - T_i), \tag{32}$$

where $\mathcal{E}_{e,i}$ are the specific internal energies; $q_{Te,Ti}$ are the thermal electron and ion fluxes; p_{Te} is thermal pressure of electrons; $\pi_i = p_{Ti} + p_v$ is the sum of the thermal and viscous pressure of the ions; the coefficient Q_{ei} determines the rate of energy exchange between electrons and ions. Because the characteristic time of electron–ion energy exchange is much greater than the pass time of plasma through the transition layer, the electron–ion relaxation can be neglected in the problem of the transition layer structure. Multiplying the equation of motion $\partial u/\partial t = -\partial(p_{Te} + \pi_i + p_r)/\partial m$ by the velocity u, and adding up the resulting equation for the kinetic energy and equations (31) and (32), we obtain an equation for the total (internal and kinetic) energy of the plasma:

$$\frac{\partial}{\partial t}\left(\mathcal{E} + \frac{u^2}{2}\right) = -\frac{\partial(pu)}{\partial m} - \frac{\partial(q_{Te} + q_{Ti})}{\partial m} - u\frac{\rho}{\rho_c}\frac{\partial}{\partial m}\left(\frac{|E|^2}{16\pi}\right), \tag{33}$$

where $p = p_{Te} + \pi_i$, and the equation for the total energy of the ions

$$\frac{\partial}{\partial t}\left(\mathcal{E}_i + \frac{u^2}{2}\right) = -\frac{\partial(\pi_i u)}{\partial m} - u\frac{\partial p_{Te}}{\partial m} - u\frac{\rho}{\rho_c}\frac{\partial}{\partial m}\left(\frac{|E|^2}{16\pi}\right) - \frac{\partial q_{Ti}}{\partial m}. \tag{34}$$

In the case of stationary motion, all quantities depend on the variables (m, t) as a combination of $\xi = m - Dt$, where $D = \rho_c c_s$ is the mass velocity of the wave. Assuming also that the temperatures T_e and T_i are constant in the transition layer, we write equation (34) in the form

$$-\rho_c c_s \frac{d}{d\xi}\left(\mathcal{E}_i + \frac{u^2}{2}\right) = \rho_c c_s$$

$$\times\left[\frac{d}{d\xi}\left(\frac{\pi_i}{\rho}\right) + \frac{1}{\rho}\frac{dp_{Te}}{d\xi} + \frac{1}{\rho_c}\frac{d}{d\xi}\left(\frac{|E|^2}{16\pi}\right)\right] - \frac{dq_{Ti}}{d\xi}. \tag{35}$$

Integrating (35) in the transition layer from ξ_0 to ξ_1 (ξ_0 corresponds to the density x_0, ξ_1 – to the density x_1) and neglecting the values of $|E|^2$ and p_v at point ξ_0 in comparison with their maximum values, we have

$$q_{Ti0} - q_{Ti1} = \rho_c c_s\left[\frac{1}{2}(u_0^2 - u_1^2) + \frac{ZT_e}{m_i}\ln\frac{\rho_0}{\rho_1}\right]$$

$$= \frac{\rho_c c_s^3}{2}\left(\frac{1}{x_0^2} - \frac{1}{x_1^2}\right) - \rho_c c_s c_{se}^2 \ln\frac{x_1}{x_0}, \tag{36}$$

where $c_{se}^2 = ZT_e/m_i$. We estimate the difference $q_{Ti0} - q_{Ti1}$ as $fn_{i0}T_i v_{Ti} = f\rho_0(T_i/m_i)^{3/2}$. Then, substituting this expression into (36), we obtain an equation for determining the ratio between the electron and ion temperatures. This value of the ion temperature should ensure the existence of a stationary transition layer. The solution of equation (36) depends on the density jump in the transition layer, which is determined by the parameter b in equation (29). For large values of the parameter b we can neglect in (36) the logarithmic term, as well as a term $1/x_1^2$ as compared to $1/x_0^2$. Then the expression for the ion temperature takes the form

$$T_i = \frac{m_i p_{r0}\Phi^2}{(2f)^{2/3}\rho_c 2\pi k_0 L}. \tag{37}$$

In this limiting case, the ion temperature is independent of the electron temperature and determined by the light pressure of the incident radiation. For small values of the parameter b in (29), when $x_0 \approx 1 - b^{1/4}$, $x_1 \approx 1 + b^{1/4}$, we can expand the quadratic and logarithmic terms in (36) in the small parameter $b^{1/4}$: $\ln(x_1/x_0) \approx 2b^{1/4}$, $(1/x_0^2 - 1/x_1^2) \approx 4b^{1/4}$. As a result, from (36) we obtain the equation for the ratio $y = T_i/(ZT_e)$

$$y^2 = h(1 + y), \tag{38}$$

where $h = (2/f)^4 T^*/(ZT_e)$, $T^* = m_i p_{r0} \Phi^2/(4\pi k_0 L \rho_c)$. Solution (38) has the form $y = (h/2)[1 + (1 + 4/h)^{1/2}]$. As an example, consider the values of $T_e = 0.55$ keV and $T_i = 20$ keV obtained in the numerical calculation; then, $y = 1.82$. This nonisothermality corresponds, according to the solution of equation (38), to the factor $f = 0.79$. It should be noted that in the numerical calculation the ions are heated not only in the transition layer, but also in the subcritical region when the plasma moves in a spatially oscillating ponderomotive potential, which modulates the plasma density and velocity profiles.

Knowing the energy of fast electrons, we can estimate the ion acceleration by the field generated by these electrons at the plasma boundary. Following [16], we define the accelerating field as

$$E = 4\pi e n_h \Delta z, \tag{39}$$

where n_h is the density of fast electrons; Δz is the distance over which electrons are emitted from the plasma. During the time $t = m_e v_h/(eE)$, the electron velocity vanishes, while the electron traverses a path $\Delta z = eEt^2/(2m_e) = m_e v_h^2/(2eE)$. Substituting this expression for Δz in (39), we obtain

$$E = (4\pi n_h \mathcal{E}_h)^{1/2}. \tag{40}$$

The expression for the flux density of fast electrons has the form

$$q_h = q_L \delta_a^r \left(\frac{R_L}{R_L + u_i \tau_L}\right)^2 = n_h v_h \mathcal{E}_h. \tag{41}$$

Determining n_h from (41) and substituting it into (40), we transform the field expression to the form

$$E = 2^{3/4}\sqrt{\pi}\left(\frac{m_e}{\mathcal{E}_h}\right)^{1/4} (q_L \delta_a^r)^{1/2} \frac{R_L}{R_L + u_i \tau_L}. \tag{42}$$

For the ion velocity $u_i = (Ze/m_i)E\tau_L$ with account for $u_i\tau_L \gg R_L$, we have

$$u_i = 2^{3/8}\left(\frac{ZeR_L}{m_i}\right)^{1/2} (\pi q_L \delta_a^r)^{1/4} \left(\frac{m_e}{\mathcal{E}_h}\right)^{1/8}. \tag{43}$$

We estimate the number of fast ions N_{ih} from the condition that the accelerating field generated by a negative charge of fast electrons is screened by a positive charge of ions with the same absolute value, $ZN_{ih} = N_{eh} = n_h \pi (R_L + u_i\tau_L)^2 \Delta z$. As a result, we obtain

$$ZN_{ih} = q_L \delta_a^r \pi R_L^2 \frac{1}{\mathcal{E}_h}\left(\frac{m_e}{8\pi e^2 n_h}\right)^{1/2}, \tag{44}$$

$$n_h = q_L \delta_a^r \left(\frac{m_e}{2}\right)^{1/2} \mathcal{E}_h^{-3/2} \left(\frac{R_L}{R_L + u_i \tau_L}\right)^2. \tag{45}$$

Let us estimate the velocity u_i for the case of a titanium target and $q_L = 10^{14}$ W cm^{-2}, $\tau_L = 20$ ns. The fraction of the resonant absorption $\delta_a^r = 0.16$ (calculated using the two-dimensional code for $\tau_L = 20$ ns), $R_L = 32.5$ μm, $\mathcal{E}_h = 78.5$ keV. For these values, we obtain from (43) $u_i = 3.68 \times 10^8$ cm s^{-1} ($\mathcal{E}_i = 3.39$ MeV).

Thus, there exist two mechanisms of ion acceleration: acceleration by the ponderomotive force and acceleration by an electric field generated by fast electrons at the plasma boundary. Acceleration by fast electrons produces a small group of high-energy ions whose energy is higher than that in the case of the ponderomotive acceleration. When the ponderomotive mechanism is used, all ions residing in the subcritical region are accelerated. Their number can be estimated as $N_{ip} = (1/m_i)\rho_c c_s \tau_L \pi R_L^2$. Finally, most ions located between the critical point and the front of the heat wave propagate at the hydrodynamic velocity. The maximum velocity is given by the expression $[2/(\gamma - 1)]c_s$ (where γ is the adiabatic exponents), and at $\gamma = 5/3$ we have $3c_s$.

4. Conclusions

Using the methods of time-of-flight diagnostics, we have measured the parameters of the ion component of plasma, recovered the function of the energy distribution of ions produced under irradiation of Mg and Pb targets by CO_2-laser pulses with a flux density of 10^{14} W cm^{-2}. We have also found groups of ions with a different effective temperature and estimated their number in the total ion flux.

We have developed an approximate analytical model of ion acceleration, which, in combination with numerical calculations by the hydrodynamic codes, makes it possible to evaluate the energy and the number of fast ions in different energy intervals. According to the model, there are different mechanisms of ion acceleration. The highest-energy and small group of the ions is accelerated by an electric field generated by fast electrons produced by resonant absorption. The group of ions that is average in number and energy is accelerated due to deformation of the density and velocity profiles under the action of the ponderomotive force in the vicinity of the critical density. The model shows that in the case of resonant absorption, the critical point is sonic; therefore, when the ponderomotive pressure greatly exceeds the thermal pressure, the subcritical plasma velocity is much higher than the sonic velocity. The largest group of ions consists of the ions accelerated by hydrodynamic expansion after the end of the laser pulse. The range of velocities of these ions varies from zero to the maximum velocity, which is several times higher than the speed of sound. The same behaviour of the energy distribution function of ions is observed in the experiment. Both in the computational model and the experimental data, there are three energy regions, where the distribution function is characterised by its own temperature. The number of ions in each group (in the experiment and model) decreases with increasing energy.

Acknowledgements. The work was performed within the framework of the scientific program of the Institute of Theoretical and Experimental Physics (State Contract No. H.4e.45.03.09.1085) and was supported by the Russian Foundation for Basic Research (Grant Nos 07-02-13602ofi_ts and 10-08-00752).

References

1. Makarov K.N., Satov Yu.A., Strel'tsov A.P., et al. *Zh. Eksp. Teor. Fiz.*, **106**, 1649 (1994).
2. Krasilnikov A.V., Makarov K.N., Satov Yu.A., et al. *Rev. Sci. Instrum.*, **72**, 1258 (2001).
3. Dubenkov V.P., Sharkov B.Yu., Golubev A.A., et al. *Laser Part. Beams*, **14**, 385 (1996).
4. Kondrashev S., Mescheryakov N., Sharkov B., et al. *Rev. Sci. Instrum.*, **71**, 1409 (2000).
5. Baranov V.Yu., Makarov K.N., Roerich V.C., et al. *Laser Part. Beams*, **14**, 347 (1996).

6. Makarov K.N., Nishchuk S.G., Rerikh V.K., et al. *Pis'ma Zh. Eksp. Teor. Fiz*., **71**, 13 (2000).
7. Stepanov A.E., Volkov G.S., Zaitsev V.I., et al. *Pis'ma Zh. Tekh. Fiz.*, **29**, 36 (2003).
8. Stepanov A.E., Satov Yu.A., Makarov K.N., et al. *Plasma Phys. Control Fusion*, **45**, 1261 (2003).
9. Satov Yu., Sharkov B., Smakovski Yu., et al. *J. Rus. Laser Res*., **25**, 524 (2004).
10. Satov Yu.A., Makarov K.N., Stepanov A.E., et al. Preprint TRINITI: 0112-A (Moscow: TsNIIatominform, 2004).
11. Satov Yu., Sharkov B., Haseroth H., et al. *J. Rus. Laser Res*., **25**, 205 (2004).
12. Silin V.P. *Parametricheskoe vozdeistvie izlucheniya bol'shoi moshchnosti na plazmy* (Parametric Action of High-Power Radiation on Plasma) (Moscow: Nauka, 1973).
13. Alexandrov A.F., Bogdankevich L.S., Rukhadze A.A. *Principles of Plasma Electrodynamics* (Heidelberg, Berlin: Springer Verlag, 1984; Moscow: Vysshaya shkola, 1978).
14. Makarov K.N., Malyuta D.D., Nishchuk S.G., et al. *Kvantovaya Elektron*., **31**, 23 (2001) [*Quantum Electron*., **31**, 23 (2001)].
15. Makarov K.N., Satov Yu.A., Smakovskii Yu.B. Preprint TRINITI: A-120 (Moscow: TsNIIatominform, 2005).
16. Gus'kov S.Yu., Demchenko N.N., Makarov K.N., et al. *Pis'ma Zh. Teor. Eksp. Fiz*., **73**, 740 (2001).
17. Ginzburg V.L. *The Propagation of Electromagnetic Waves in Plasma* (Oxford: Pergamon, 1970; Moscow: Nauka, 1967); Denisov N.G. *Zh. Eksp. Teor. Fiz*., **31**, 609 (1956); Gildenburg V.B. *Zh. Eksp. Teor. Fiz*., **46**, 2156 (1964).
18. Freidberg J.P., Mitchell R.W., Morse R.L., Rudsinski L.I. *Phys. Rev. Lett.*, **28**, 795 (1972).
19. Braginsky S.I. *Voprosy teorii plasmy* (Problems of Plasma Theory). Ed. by M.A. Leontovich (Moscow: Gosatomizdat, 1963) Vol. 1, p. 183.
20. Lifshits E.M., Pitaevskii L.P. *Physical Kinetics* (New York: Pergamon Press, 1981; Moscow: Nauka, 1979).
21. Demchenko N.N., Rozanov V.B. *Proc. SPIE Int. Soc. Opt. Eng*., **5228**, 427 (2003).
22. Lebo I.G., Demchenko N.N., Iskakov A.B., Limpouch J., Rozanov V.B., Tishkin V.T. *Laser Part. Beams*, **22**, 267 (2004).